Atmos. Chem. Phys. Discuss., 8, 16713–16762, 2008
www.atmos-chem-phys-discuss.net/8/16713/2008/

Atmospheric Chemistry and Physics Discussions

This discussion paper is/has been under review for the journal *Atmospheric Chemistry and Physics (ACP)*. Please refer to the corresponding final paper in *ACP* if available.

Tropospheric NO_2 column densities deduced from zenith-sky DOAS measurements in Shanghai, China, and their application to satellite validation

D. Chen[1], B. Zhou[1], S. Beirle[2], L. M. Chen[1], and T. Wagner[2]

[1]Department of Environmental Science and Engineering, Fudan University, China
[2]Max Planck Institute for Chemistry, Mainz, Germany

Received: 20 June 2008 – Accepted: 11 August 2008 – Published: 3 September 2008

Correspondence to: D. Chen (052047006@fudan.edu.cn)

Published by Copernicus Publications on behalf of the European Geosciences Union.

Abstract

Zenith-sky scattered sunlight observations using differential optical absorption spectroscopy (DOAS) technique were carried out in Shanghai, China (31.3° N, 121.5° E) since December 2006. At this polluted urban site, the measurement provided NO_2 total columns in the daytime. Here, we present a new method to extract time series of tropospheric vertical column densities (VCD) of NO_2 from these observations. The derived tropospheric NO_2 VCD is an important quantity for the estimation of emissions and for the validation of satellite observations. Our method makes use of assumptions on the relative NO_2 height profiles and on the diurnal variation of the stratospheric NO_2 VCD. The influence of these parameters on the retrieved tropospheric NO_2 VCD is discussed; for a polluted site like Shanghai, the accuracy of our method is estimated to be <20% for solar zenith angle (SZA) lower than 85°. From simultaneously performed long-path DOAS measurement, the NO_2 surface concentration at the same site was observed and the corresponding tropospheric NO_2 VCD was estimated using the assumed seasonal NO_2 profiles in the planetary boundary layer (PBL). By making a comparison between the tropospheric NO_2 VCD from zenith-sky and long-path DOAS measurements, it was found that the former provided more realistic information about total tropospheric pollution than the latter, so it's more suitable for satellite data validation than the in situ measurement. A comparison between the tropospheric NO_2 VCD from ground-based zenith-sky measurement and SCIAMACHY was also made. Satellite validation for a strongly polluted area is highly needed, but exhibits also a great challenge. Our comparison showed good agreement, considering in particular the different spatial resolutions between the two measurements.

1 Introduction

Nitrogen dioxide is one of the most important trace gases in tropospheric chemistry. It directly participates in the photochemical formation of tropospheric ozone and con-

ACPD

8, 16713–16762, 2008

tributes locally to radiative forcing. The main NO_x (NO_2+NO) sources include both anthropogenic and natural emissions, such as fossil fuel combustion, biomass burning, lightning and soil emission. Considering the importance of NO_2 to human health and atmospheric chemistry, there have been many ground-based, air-borne and space-borne instruments carrying out NO_2 observations. In situ sampling using chemiluminescence technique has been adopted as a routine monitoring method to measure NO_2 concentration near the ground. With the development of remote sensing techniques, especially the differential optical absorption spectroscopy (DOAS), the total amount of NO_2 in the atmosphere can be acquired either from space or ground. After the launch of ERS-2 in 1995, the global distribution of total and tropospheric NO_2 is mapped by the Global Ozone Monitoring Experiment (GOME) (Burrows et al., 1999b) which helps to improve the knowledge of atmospheric pollution and its transportation. Additional satellite instruments were launched since then, continuing the GOME time series: in 2002 the SCanning Imaging Absorption spectroMeter for Atmospheric CHartographY (SCIAMACHY) was launched on ENVISAT (Bovensmann et al., 1999); in 2004 the Ozone Monitoring Instrument (OMI) was launched on AURA (Levelt and Noordhoek, 2002); in 2006 the first GOME-2 instrument (in total three instruments are scheduled) was launched on METOP (EUMETSAT, 2008).

Ground-based instruments (like e.g. Systeme d'Analyse par Observations Zenithales, SAOZ or similar UV/vis instruments) (see e.g. Noxon, 1975) installed at a number of NDSC stations over the globe continuously provide total NO_2 columns for trend analysis and satellite data validation (Pommereau and Goutail, 1988; Ionov et al., 2006a). Moreover, as an advanced improvement of Zenith-sky DOAS, Multi AXis Differential Optical Absorption Spectroscopy (MAXDOAS) instrument was developed to retrieve vertical profile of NO_2 concentration, as well as tropospheric and stratospheric columns, so it is suitable for the validation of satellite tropospheric data (Hönninger and Platt, 2002; Heue et al., 2005; Celarier et al., 2008; Brinksma et al., 2008).

Richter et al. (2005) reported a significant increase of tropospheric NO_2 column over East Central China from 1996–2004 observed by GOME and SCIAMACHY. By attribut-

ACPD
8, 16713–16762, 2008

ing such increase to the growth of NO_x emission, the authors pointed out the necessity of detailed inventory studies to confirm satellite data. However, considering the sensitivity of satellite observation to pollution located near the ground, as well as the uncertainties contained in satellite retrieval process (Boersma et al., 2004), it seems necessary to carry out both in situ and ground-based measurements in east central China to investigate the tropospheric pollution status and validate satellite observations. Ground-based instruments can in particular yield additional valuable information on finer spatial scales and about the diurnal variation.

For this purpose, zenith-sky DOAS and long-path DOAS measurements were performed in Shanghai, China (31.3° N, 121.5° E). By combining these two observations, both the tropospheric column and surface concentration of NO_2 can be acquired. In contrast to previous studies, which measured only twilight NO_2 columns (e.g. Petritoli et al., 2004; Ionov et al., 2006b), the present study observed zenith-sky scattered light during the whole day and retrieved the diurnal variation of the total NO_2 column. By using some simple but rational assumptions, the tropospheric NO_2 column was extracted from the total one. Such study provides comprehensive information about surface emission and total tropospheric pollution, which is necessary for satellite data validation and total emission investigation. A comparison between the two measurement results (zenith-sky and long-path DOAS) can also give us some indications about the diurnal variation of planetary boundary layer (PBL) height.

The paper is organized as follows: in the next section both ground-based DOAS instruments (zenith-sky and long-path) are described. In Sect. 3, the determination of the tropospheric NO_2 vertical column from these observations is outlined. Section 4 presents a comparison between both ground-based data sets and finally with satellite observations.

ACPD
8, 16713–16762, 2008

2 Ground-based instruments and spectral analysis

2.1 Zenith-sky measurement

2.1.1 Experiments and instruments

Ground-based observation of zenith-sky scattered sunlight was firstly performed from 16 December 2006 to 18 December 2006 at Chongming Island (31.5° N, 121.8° E), which lies to the northeast of Shanghai, borders on the Pacific Ocean, and is located at the estuary of Yangtze River. Considering the geographical location of this island and the few industries on it, it can be concluded as the most suitable rural site around Shanghai with small tropospheric NO_2 pollution. The recording of zenith-sky scattered sunlight was performed automatically when the solar zenith angle (SZA) was below 92°.

After the three-day experiment, the instruments were moved to Fudan University (31.3° N, 121.5° E), carrying out continuous ground-based measurements since 22 December 2006. Located near the middle circle viaduct of Shanghai, this urban site suffers from heavy traffic pollution. The NO_2 absorption signal can be easily detected in the spectra, in which the contribution of the tropospheric part is usually much larger than the stratospheric one, especially at small SZA. The instruments mounted on the top roof stairs of a 20 m tall building comprised three parts, including a telescope, a spectrometer and a PC. The scattered sunlight was received by a telescope with 46 mm diameter and 300 mm focal length, and led to spectrometer via quartz fiber. The HR4000 high resolution fiber optic spectrometer (Ocean Optics, Inc.) was used to acquire UV-visible zenith-sky spectra with a 1200 grooves/mm grating and a 100 μm-width entrance slit, which yielded a full-width half-maximum (FWHM) resolution of about 0.73 nm. The detector is a linear CCD array with 3648 pixels (each 8 μm×200 μm). A PC controlled the automatic measurements and stored the spectra. The offset was removed automatically during the spectra recording process. The signal of dark current was measured every night and subtracted from each spectrum according to the cor-

responding average exposure time. Depending on the intensity of received scattered sunlight, the exposure time was adjusted automatically to maximize the total signal. Simultaneously, the number of accumulations comprising a spectral set also varied to restrict the average time interval between two spectra to about 5 min. The spectral wavelength range is 345–565 nm.

2.1.2 NO_2 total column retrieval

The NO_2 column density was retrieved by means of Differential Optical Absorption Spectroscopy (DOAS) (Platt, 1994), using the spectral region between 434 nm and 462 nm. The WinDOAS-software (Fayt and Roozendael, 2001) was applied to analyze the zenith-sky spectra. The logarithm of a Fraunhofer reference spectrum (which was recorded at noon of a clear day) as well as several trace gas absorption cross sections were fitted to the logarithm of each measured spectrum by means of a non-linear least squares fitting routine (allowing shift and squeeze of the fitted spectra). Also a low order polynomial (representing the slow variation contribution of broad-band absorption, as well as the Rayleigh and Mie scattering processes) and a Ring spectrum (calculated by WinDOAS) were included. The cross sections of NO_2 (Burrows et al., 1998), O_3 (Burrows et al., 1999a), O_4 (Greenblatt et al., 1990), and H_2O from HITRAN (Rothman, 1998) were taken into account. The cross sections for NO_2 and O_3 at 223 K and 293 K were used and orthogonalized to account for the partitioning between the (warm) troposphere and (cold) stratosphere of these two trace gases. As result of the DOAS analysis, the differential slant column density (DSCD) of NO_2 was retrieved, which is the difference between the NO_2 slant column densities (SCD, the integrated trace gas concentration along the absorption path) of the measured spectrum and the Fraunhofer reference spectrum.

2.2 Long-path DOAS measurement

In order to get the information about the NO_2 surface concentration, a set of long-path DOAS equipment was installed at the same location as the zenith-sky instruments. Detailed description of the instruments can be found in Yu et al. (2004). In short, the collimated beam of white light from a 150 W Xe short-arc lamp was transmitted by a co-axial telescope to the open atmosphere and folded back into the telescope by an array of quartz corner cube retroreflectors, which was mounted at a distance of 507 m east of the experimental building and the same altitude as the telescope. Led by a quartz fiber, the light entered a spectrometer. Spectra in 372–444 nm was recorded by a Czerny-Turner spectrograph with a focal length of 0.3 m, and detected by a 1024-pixel photodiode array detector cooled to −15°. With a fixed number of 20 scans (with an individual exposure time from 5 to 30 s), the average time resolution is about 4 minutes, which is similar to that of the zenith-sky measurement. The average NO_2 concentration along the optical path was analyzed using the DOASIS software package (Kraus, 2001) in the spectral region of 424–435 nm, with the cross sections of NO_2 (Burrows et al., 1998) and O_3 (Burrows et al., 1999a) at 293 K, as well as the "background Fraunhofer structure" induced by the scattered sunlight received by the telescope (Zhou et al., 2005) taken into account. The retrieved amount was taken as the NO_2 surface concentration ($C_{surface}$) at the experimental site.

3 Deduction of the tropospheric NO_2 VCD from ground-based instruments

3.1 Tropospheric NO_2 VCD derived from zenith-sky observation

As mentioned in Sect. 2.1.2, the differential slant column density (DSCD) of NO_2 retrieved from zenith-sky measurement is the difference between total NO_2 columns contained in the measured and Fraunhofer reference spectra. In order to extract the tropospheric NO_2 vertical column density (VCD), there are three steps that should be

ACPD
8, 16713–16762, 2008

followed:

1. The NO_2 SCD in the reference spectrum (SCD_{ref}) is added to the retrieved DSCD to derive the total SCD in the measured spectra (SCD_{total});

2. The stratospheric NO_2 SCD (SCD_{strato}) is subtracted from the total one to get the tropospheric NO_2 SCD (SCD_{tropo});

3. The tropospheric NO_2 SCD (SCD_{tropo}) is divided by corresponding tropospheric air mass factor (AMF) to get the tropospheric NO_2 VCD (VCD_{tropo_zenith}) from zenith-sky measurement.

The strategy can be described by Eq. (1)–(3) as below:

$$SCD_{total} = DSCD + SCD_{ref} \quad (1)$$

$$SCD_{tropo} = SCD_{total} - SCD_{strato} \quad (2)$$

$$VCD_{tropo\_zenith} = SCD_{tropo} / AMF_{tropo} \quad (3)$$

To perform these steps, several parameters have to be determined, including the tropospheric and stratospheric NO_2 AMF (AMF_{tropo} and AMF_{strato}), SCD_{ref} and SCD_{strato} as described in the following sections. For that purpose, some assumptions were made; the NO_2 surface concentration acquired by long-path DOAS measurement was also used.

3.1.1 Separation of the stratospheric NO_2 column density

For practical reasons, here we do not strictly follow the order described above (Eq. 1–3). Instead, step 1 will be described in Sect. 3.1.3, because it makes use of quantities defined in the current section. The observation of stratospheric NO_2 column is possible during the twilight period, in which the sensitivity of zenith-sky instruments is greatly enhanced as the result of long light path in stratosphere while short path in troposphere.

ACPD
8, 16713–16762, 2008

When the sun is low, the stratospheric AMF is much larger than the tropospheric one, which is always close to unity except for the case of tropospheric cloud existence (e.g. Wagner et al., 1998; Pfeilsticker et al., 1998). Therefore, our first idea was to retrieve daily stratospheric NO_2 columns from sunrise and sunset spectra at SZA near 90°. However, as Roozendael et al. (1994) pointed out, even during twilight period, the pollution episodes near the ground can significantly increase the measured total absorption and thus introduce large errors in the observation of stratospheric NO_2. Unfortunately, this is the case at the present urban site, which always suffers from heavy traffic pollution. The perturbation caused by tropospheric NO_2 to the twilight retrieval results is illustrated in Fig. 1. It shows the diurnal variation of NO_2 DSCD on 2 February 2007 with a reference spectrum measured at noon on 26 February 2007 (clear day). The non-U-shape variation of NO_2 DSCD indicates a strong interference of tropospheric NO_2 pollution. Because such influence is always large in the urban site, the twilight data fail to provide the information about the stratospheric NO_2 column.

Instead, the three-day zenith-sky observation at Chongming Island serves for this aim. Figure 2 shows the measured NO_2 DSCD in 17 December 2006 with a reference spectrum taken at local noon of the same day. The U-shape variation suggests a low or constant tropospheric NO_2 amount. Considering the meteorological condition of that day, including sea wind with high speed and the observation of a clear sky with high visibility, the NO_2 concentration in the boundary layer must be very low. Therefore, we used these observations to estimate the stratospheric NO_2 SCD. First, the stratospheric NO_2 VCD (VCD_{strato}) was deduced from the twilight measurements with the equations below:

$$DSCD = SCD_{mea} - SCD_{ref} = VCD_{strato} \times AMF_{mea} - VCD_{strato} \times AMF_{ref} \quad (4)$$

$$VCD_{strato} = DSCD / DAMF \quad (5)$$

where SCD_{mea} and SCD_{ref} are the NO_2 SCD in the measured and reference spectra respectively; while AMF_{mea} and AMF_{ref} are the corresponding stratospheric AMF

ACPD
8, 16713–16762, 2008

(see Sect. 3.1.2); DAMF is the difference between AMF_{mea} and AMF_{ref}. The diurnal variation of stratospheric NO_2 VCD was ignored in Eq. (4) and (5); however, the corresponding errors are only small, because for large SZA, AMF_{mea} is typically much larger than AMF_{ref}. By averaging the VCD_{strato} between 88–90° SZA, the a.m. and p.m. stratospheric NO_2 vertical column densities were derived, which are 2.88×10^{15} molecule cm^{-2} and 4.02×10^{15} molecule cm^{-2} respectively.

According to Lambert et al. (2002), the typical NO_2 cycle in the daytime displays a quasi-linear slow increase due to the NO_2/NO photochemical equilibrium and photolysis of N_2O_5. Therefore, the diurnal NO_2 stratospheric VCD can be estimated by making a linear interpolation between the a.m. and p.m. VCD_{strato} over the whole day. Finally, by multiplying VCD_{strato} by the corresponding stratospheric AMF, the SCD_{strato} were derived. These SCD_{strato} were then used in Eq. (2).

The SCD_{strato} calculated in this way were taken as the typical stratospheric columns in Shanghai from 22 December 2006 to 31 March 2007, and used to deduce the tropospheric VCD from observations at the urban site. The underlying assumption of spatial and temporal invariance of stratospheric NO_2 is certainly an error source in the extraction process. However, for polluted areas, the uncertainty caused by the stratospheric part should be rather small (especially for small SZA). In order to reduce this error, another two pairs of a.m. and p.m. stratospheric values (3.70×10^{15} molecule cm^{-2} and 5.93×10^{15} molecule cm^{-2}, 2.58×10^{15} molecule cm^{-2} and 5.61×10^{15} molecule cm^{-2} respectively) measured at the urban site during twilight periods on 22 May 2007 and 17 September 2007 were chosen to process data from April to July and August to December 2007, respectively. These two days are also characterized by ideal meteorological condition and low surface NO_2 concentration (demonstrated by the long-path DOAS measurement data).

3.1.2 Calculation of the stratospheric and tropospheric AMF

The stratospheric and tropospheric NO_2 AMF in this study for SCD and VCD conversion were calculated with the radiative transfer model TRACY-II (Deutschmann and

ACPD
8, 16713–16762, 2008

Wagner, 2006; Wagner et al., 2007), in which the radiative transfer equation (RTE) is solved in a spherical three dimensional slice of the atmosphere, using the backward Monte Carlo formalism. Clouds and aerosol above 2 km were not included in the simulation. The surface albedo was set to 0.18. The monthly and latitudinal-averaged vertical profiles for pressure, temperature and ozone at 30° N–40° N were taken from the McLinden climatology contained in SCIATRAN database (Institute of Remote Sensing University of Bremen, 2004). In AMF calculation, the NO_2 vertical profile is a key parameter affecting the results. For the stratospheric AMF, the NO_2 profiles in McLinden climatology were used with no NO_2 below 2 km. While for the tropospheric AMF, the assumed seasonal NO_2 profiles representing winter (December, January and February), spring (March, April and May), summer (June, July and August) and autumn (September, October and November) respectively were adopted with constant tropospheric NO_2 concentration (5.38×10^{11} molecule cm^{-3}, equal to 20 ppb at the ground level) within the PBL, which extends to different altitudes according to the seasons. The aerosol was assumed to be located at the same altitude range as the tropospheric NO_2, with the uniform asymmetry parameter (0.68) and single scattering albedo (SSA, 1) for all seasons. According to Duan and Mao (2007), the maximum atmospheric aerosol optical depth (AOD) over the Yangtze River Delta occurred in summer, followed by spring, autumn and the minimum value in winter. Therefore, we adopted the similar seasonal aerosol scenarios in TRACY-II (see Table 1) and modeled the corresponding seasonal tropospheric NO_2 AMF, as shown in Fig. 3.

However, it is important to note that due to the changes of meteorological and pollution conditions, in reality the PBL height and AOD do not remain constant, neither does the tropospheric AMF. The uncertainties caused by the tropospheric NO_2 profile, aerosol settings, as well as the PBL height are discussed in Sect. 4.1.1

ACPD
8, 16713–16762, 2008

3.1.3 Determination of NO_2 SCD in the reference spectrum

The SCD in the reference spectrum can be divided into the stratospheric and tropospheric parts.

$$SCD_{ref}=SCD_{strato\_ref}+SCD_{tropo\_ref} \quad (6)$$

The derivation of the former had been described in Sect. 3.1.1. The latter was determined by the equation below:

$$SCD_{tropo\_ref}=VCD_{tropo\_ref}\times AMF_{tropo\_ref} \quad (7)$$

The calculation of tropospheric VCD in the reference spectrum (VCD_{tropo_ref}) was performed using the surface concentration measured by long-path DOAS experiment. From the assumed NO_2 profiles (as described in Sect. 3.1.2), the corresponding tropospheric VCD can be calculated by multiplying the NO_2 concentration at the bottom of the profiles by the height of PBL. Therefore, for the tropospheric VCD in the reference spectrum, it was derived by using the average NO_2 concentration observed by long-path DOAS measurement.

Here, the average of 5 surface concentration data measured around the time when the reference spectrum was recorded was multiplied by the assumed seasonal PBL heights to deduce the tropospheric NO_2 VCD in the reference spectrum. It should be noted that a single Fraunhofer reference spectrum was used for the analysis of a large period of time. Thus the potential errors in the determination of SCD_{ref} would affect all observations in a similar way. Thus, in particular the relative variation of the derived tropospheric VCD does hardly depend on the determined absolute value of SCD_{ref}.

With the above parameters, the tropospheric NO_2 vertical columns were finally extracted from the zenith-sky observations. Figure 4 shows the deduction process of the diurnal VCD_{tropo_zenith} on 2 February 2007, including the variation of the total SCD (SCD_{total}), the stratospheric SCD (SCD_{strato}) (Fig. 4a), the tropospheric SCD (SCD_{tropo}) (Fig. 4b) and the deduced tropospheric VCD (VCD_{tropo_zenith}) (Fig. 4c). Comparing Fig. 4c with Fig. 4a, we can find that the tropospheric VCD and total SCD display the

ACPD
8, 16713–16762, 2008

same variation trend, which indicates the dominance of the tropospheric part in the total column, as well as a severe pollution in lower atmosphere.

3.1.4 Error estimation

This section provides a summary on the error estimation for the tropospheric NO_2 VCD derived from the zenith looking instruments; it is based on several detailed investigations, which, for practical reasons, are presented in Sect. 4.1, where the results of both ground-based instruments are compared. According to the above three steps, there are three main error sources which could influence the correctness of the extraction results.

1. The deduction of stratospheric SCD. Firstly, as discussed in Sect. 3.1.1, we used a linear interpolation between the a.m. and p.m. stratospheric NO_2 VCD to calculate the diurnal variation of stratospheric SCD. Secondly, there were three pairs of a.m. and p.m. stratospheric VCD adopted, one was deduced from the experiment at Chongming Island, the other two from clear-day observations at the urban site. Here by using these three pairs of stratospheric VCD to analyze data recorded during one year period, the spatial and temporal variance of stratospheric NO_2 was ignored, which inevitably introduced uncertainties. However, as mentioned before, for the polluted area, the proportion of stratospheric NO_2 column to the total column is greatly reduced, especially for small SZA. For the measurements analyzed here, the respective error is estimated to be about 2×10^{15} molecule cm^{-2} (typically <10%) for SZA <85°.

2. Tropospheric and stratospheric AMF. As discussed by Bassford et al. (2001), different RT model parameterizations, including the vertical profiles of the absorbers, surface albedo, aerosol, cloud and other model parameters, contributed to the uncertainties of the resulting AMF. For tropospheric AMF calculation, the assumed seasonal NO_2 profiles and aerosol scenarios were adopted here with an additional assumption that tropospheric NO_2 and aerosol were located at the same

ACPD
8, 16713–16762, 2008

altitude range with the same shape of profile (the influence of the location of tropospheric NO_2 and aerosol layers, different aerosol properties, as well as the PBL height settings on the resulting tropospheric AMF was investigated in more detail in Sect. 4.1.1 and 4.1.2). The error caused by the uncertainties of AMF is estimated to be < 15% for most cases.

3. The determination of tropospheric NO_2 VCD in the reference spectrum (VCD_{tropo_ref}). As described in Sect. 3.1.3, the deduction of VCD_{tropo_ref} involves the conversion of NO_2 surface concentration into tropospheric VCD by using the assumed PBL heights defined in the seasonal tropospheric NO_2 profiles. Therefore, the uncertainties of the tropospheric NO_2 profile settings also affect VCD_{tropo_ref}. However, as the reference spectra used here were recorded at local noon and with only slight tropospheric NO_2 pollution, the VCD_{tropo_ref} itself is too small to substantially influence the retrieved tropospheric NO_2 VCD (VCD_{tropo_zenith}). The respective error of the retrieved tropospheric NO_2 VCD is estimated to be <5%.

In total, the error of the analyzed tropospheric NO_2 VCD derived from zenith-sky DOAS measurement is typically <20% for SZA <85°. It should be noted that this error estimate is only valid for clear skies; in the presence of clouds or heavy aerosol loads, the error might be substantially larger (see Sect. 4.1).

3.2 Tropospheric NO_2 VCD derived from long-path DOAS observation

In order to validate the extraction results, the hourly-averaged NO_2 surface concentration measured by long-path DOAS observation was also converted into the corresponding tropospheric VCD ($VCD_{tropo\_surface}$) by multiplying the assumed seasonal PBL height, and compared with the hourly-averaged VCD_{tropo_zenith}. It is interesting to note that, in contrast to the VCD_{tropo_zenith}, errors in the $VCD_{tropo\_surface}$ as a result of a wrong PBL height setting are directly proportional to the errors of the PBL height.

ACPD
8, 16713–16762, 2008

4 Results and discussion

In this section, the resulting tropospheric NO_2 VCD derived from zenith-sky measurement were firstly compared with the VCD converted from the surface concentration. Then factors affecting the comparison were explored and discussed. Finally, a comparison between the tropospheric NO_2 VCD derived from SCIAMACHY observation and ground-based observations was presented.

4.1 Comparison between the tropospheric NO_2 VCD deduced from zenith-sky and long-path DOAS measurements

Before the comparison, the potential influence of tropospheric clouds should be discussed. As demonstrated by Wagner et al. (1998) and Pfeilsticker et al. (1998), the photon diffusion in optical thick clouds and the multiple reflections between layers and patches of clouds can greatly enhance the light path. If there is NO_2 located at the cloud level, the absorption would become much larger than that for clear sky condition. On the other hand, in the presence of high thin clouds, the tropospheric absorption can also be slightly decreased. If in cloudy conditions, the tropospheric AMF calculated under cloud-free assumption are used to retrieve the tropospheric VCD, large errors can occur. Without the information about the location and extension of clouds, as well as the distribution of NO_2 inside clouds, it is difficult to correctly extract the tropospheric NO_2 VCD from zenith-sky measurement. Therefore, in this study, only the results for clear days were selected for comparison. Here the daily meteorological observations and the diurnal variation of the retrieved O_4 column were combined to select days in which the cloud impact can be neglected. Because the O_4 concentration in the atmosphere mainly depends on the square of the O_2 concentration, and the atmospheric O_2 column varies only slightly (depending on pressure) (Perner and Platt, 1980; Greenblatt et al., 1990; Wagner et al., 2002; Wittrock et al., 2004), the O_4 absorption can be used as a criterion to identify the existence of clouds and aerosols. For a trace gas with constant amount in the atmosphere, the observed diurnal SCD variation shows a

ACPD
8, 16713–16762, 2008

smooth increase with the increasing SZA in clear sky condition (Meena et al., 2004). Therefore, here the U-shape diurnal variation of the retrieved O_4 DSCD was taken as an indicator for a clear day. As shown in Fig. 5, using this criterion, it can well be distinguished between a clear day (30 May 2007) and a cloudy day (31 May 2007). Following the above criteria, data from 98 days under cloud-free condition during 22 December 2006 and 31 December 2007 were chosen for comparison. The results were separated into four groups. Figure 6 shows the typical examples for the selected days of each group. In the first group (including 12 days), both the hourly-averaged values and relative diurnal variations of the tropospheric NO_2 VCD derived from zenith-sky observation (VCD_{tropo_zenith}) and long-path DOAS observation ($VCD_{tropo\_surface}$) present good agreements. In the second group (including 25 days), only the relative variations of VCD_{tropo_zenith} and $VCD_{tropo\_surface}$ agree. In the third group (including 33 days), VCD_{tropo_zenith} and $VCD_{tropo\_surface}$ have different values and relative variations. In the last group (including 28 days), the curves of diurnal VCD_{tropo_zenith} and $VCD_{tropo\_surface}$ intersect, but with different relative variations. As there were only one third of the days belonging to the first and second groups, the VCD_{tropo_zenith} and $VCD_{tropo\_surface}$ do not agree well.

The overall regression analysis of $VCD_{tropo\_surface}$ and VCD_{tropo_zenith} for cloud-free observations from 98 days was performed. Since there are uncertainties in both data sets, the standard least-squares method, which only minimizes the distances between the fitted line and the data in the y-direction, is not appropriate. Here a weighted bivariate least-squares method (Eqs. 5 and 6 in Cantrell, 2008), which considers the errors in both y- and x-variables, and minimizes the perpendicular distances between the fitted line and the data, was adopted. Such algorithm allows assigning individual uncertainties to all data points. Therefore, an absolute plus a relative uncertainty of both measurements were estimated and applied to the regression. For VCD_{tropo_zenith}, the error is estimated to be $2\times10^{15}\pm20\%$; For $VCD_{tropo\_surface}$, the assumptions on the PBL height and on the homogenous mixing within the PBL are the dominant error sources. Thus, a relative error of about 40% is estimated (see also sections below).

ACPD
8, 16713–16762, 2008

Using these assumptions, the fitted regression line, shown in Fig. 7, indicates a rather low correlation between the two data sets (R=0.50).

As mentioned in Sect. 3, the standardized seasonal shapes of NO_2 profile were adopted to convert the surface concentration into the tropospheric VCD ($VCD_{tropo\_surface}$). However, due to the change of the meteorological condition during the day, the PBL height does not remain constant, especially in the situation of temperature inversion. Daily comparison of $VCD_{tropo\_surface}$ and VCD_{tropo_zenith} always showed higher $VCD_{tropo\_surface}$ in the morning, which indicates an overestimate of the PBL height. Figure 8 shows the monthly-averaged diurnal PBL height for Shanghai in October and December 2006, modeled and provided by Patrick Jöckel, modeling group at MPI for Chemistry, Mainz, Germany (The model results were taken from the S2 simulation of the Modular Earth Submodel System (MESSy), see Jöckel et al., 2006). The PBL height fluctuates sharply from 06:00 LT to 11:00 LT, and then remains relatively unchanged until 18:00 LT. In order to investigate the influence of PBL height variation in more detail, the time from 06:00 LT to 19:00 LT every day is divided into 3 periods, which are 06:00~11:00 LT, 11:00~15:00 LT and 15:00~19:00 LT respectively. The orthogonal regression analysis of $VCD_{tropo\_surface}$ and VCD_{tropo_zenith} in each period is shown in Fig. 9. As expected, the best correspondence happens in the second period, from 11:00 LT to 15:00 LT, in which the PBL height is more constant compared with the other two periods, and the influence of uncertainties caused by the stratospheric NO_2 VCD deduction is minimized because of the small SZA. In addition, the correlation between $VCD_{tropo\_surface}$ and VCD_{tropo_zenith} in the third period is better than that in the first period, which further demonstrates the influence of PBL height variation on the comparison results.

4.1.1 The influence of aerosol settings and profile assumptions on the tropospheric AMF

As mentioned in Sect. 3, the tropospheric NO_2 and aerosol profiles are key parameters in the AMF simulation. Concretely, the uncertainties are induced by the settings of PBL

ACPD
8, 16713–16762, 2008

height, aerosol properties (AOD, single scattering albedo, asymmetry parameter), as well as the assumption that the tropospheric NO_2 and aerosol layers are located within the same altitude range. Considering such assumption is the most feasible one we can make here (the possible location and extension of tropospheric NO_2 and aerosol layers are too variable to be comprehensively included in this study), in order to assess the potential influence of varying layer heights, here we assume two cases (case 1 and 3 as shown in Table 2) with tropospheric NO_2 and aerosol layers extending to different altitudes, and compare the deduced tropospheric AMF with those modeled under the assumption of tropospheric NO_2 and aerosol located within the same altitude range (case 2 and 4 as shown in Table 2).

Figure 10a and b show the tropospheric AMF deduced under the assumptions that the aerosol layer extends lower (case 1 and 2) and higher (case 3 and 4) than the tropospheric NO_2, respectively. Because of the multiple scattering effect of aerosol, when the top of aerosol layer is located above tropospheric NO_2, a greater fraction of the observed photons would pass the NO_2 layer on a vertical rather than on a slant path (depending on the SZA). Thus, the deduced tropospheric AMF would be reduced, especially for SZA larger than 70° (see Fig. 10b). Similarly, the tropospheric AMF can be enhanced if the top of aerosol layer falls below that of tropospheric NO_2 (see Fig. 10a). Since the dominant fraction of VCD_{tropo_zenith} were observed at small SZA, the assumption of the relative location of tropospheric NO_2 and aerosol layers would not cause large error to the deduction results.

Secondly, in order to investigate the influence of aerosol single scattering albedo (SSA) on the derived tropospheric AMF, we also tested cases 5 and 6 (see Table 2) with single scattering albedo set to 0.95 and 0.9, respectively. Combining with case 4, it is concluded that the tropospheric AMF increases with the increasing single scattering albedo (as shown in Fig. 10c). Since 0.95 is probably the most realistic value of aerosol single scattering albedo, the errors caused by an assumed uncertainty of the single scattering albedo in the range of 0.9 to 1 are below 10% for SZA lower than 85°.

Thirdly, the influence of AOD settings on the tropospheric AMF is also investigated.

ACPD
8, 16713–16762, 2008

Under the conditions of four different AOD (0.4, 0.8, 1.2 and 1.5, respectively), with the tropospheric NO_2 and aerosol both located within 0–0.8 km (see case 7, 8, 4 and 9 in Table 2), the tropospheric AMF modeled by TRACY-II were shown in Fig. 10d. For SZA lower than 85°, the AMF under all AOD assumptions agree within about 10%. Moreover, the four groups of AMF almost agree during the SZA range from 75° to 85°. For SZA below 75°, the AMF enhances with the increasing AOD, which also demonstrates the multiple scattering effect of aerosol on solar radiance. However, considering the level of deviations, the uncertainties of AOD assumption would not cause significant error to the deduced VCD_{tropo_zenith}.

Finally, we investigate the influence of PBL height on the modeled tropospheric AMF. Two additional PBL heights with the top of PBL located at 0.3 km and 0.6 km were defined (see case 10 and 11 in Table 2). Together with the PBL heights of 0.8 km and 1 km (case 4 and 2, respectively), four cases with those different PBL height assumptions were input into TRACY-II with the AOD set to 1.2 (different aerosol extinction coefficient in each aerosol profile). The corresponding tropospheric AMF are shown in Fig. 10e. The influence of PBL height variation on the tropospheric AMF is nearly negligible. Thus, it can be concluded that as long as the tropospheric NO_2 and aerosol are located at the same altitude range with a constant AOD, the corresponding tropospheric AMF hardly varies with the top of PBL.

In conclusion, from the above discussions, though the respective uncertainties in each group of cases are around 10% for large SZA, the overall errors of tropospheric NO_2 AMF caused by the uncertainties of aerosol properties, as well as the aerosol and NO_2 profile settings in TRACY-II can be estimated to be within 15% for SZA lower than 70°, which corresponds to the error estimation in Sect. 3.1.4.

4.1.2 The influence of PBL height variation on the VCD_{tropo_zenith} and $VCD_{tropo\_surface}$ calculations

Figure 11a and b show the VCD_{tropo_zenith} and $VCD_{tropo\_surface}$ in 9 June 2007, deduced under the four PBL height assumptions defined in the previous section.

ACPD
8, 16713–16762, 2008

The much larger deviation for the different profiles of $VCD_{tropo\_surface}$ than that for VCD_{tropo_zenith} demonstrates the big uncertainties of the conversion from surface concentration to $VCD_{tropo\_surface}$. Thus one important conclusion of this comparison is that VCD_{tropo_zenith} is more reliable and probably more suitable for satellite validation. However, it should be pointed out that because the calculation of VCD_{tropo_ref} also involves the conversion of NO_2 surface concentration into tropospheric VCD using the PBL height information, it is important to choose a "clean" Fraunhofer reference spectrum, in which the NO_2 pollution in lower atmosphere is slight, to reduce the proportion of VCD_{tropo_ref} to the deduced VCD_{tropo_zenith}, and thus to enhance the reliability of VCD_{tropo_zenith}.

In addition, the comparison between VCD_{tropo_zenith} and $VCD_{tropo\_surface}$ deduced under the above different PBL height assumptions is made (see Fig. 12). The different extent of agreement in each group strongly indicates the validity of their PBL height settings in certain period of time (see also Fig. 8). Thus, from the comparison between VCD_{tropo_zenith} and $VCD_{tropo\_surface}$ on clear days, valuable information about the real PBL height can be derived, which should be investigated in more detail in the future.

4.2 Comparison with SCIAMACHY tropospheric NO_2 VCD

4.2.1 SCIAMACHY instrument and data analysis

SCIAMACHY (SCanning Imaging Absorption spectroMeter for Atmospheric CHartography) is an 8 channel spectrometer aboard the European Space Agency's (ESA) Environmental Satellite (ENVISAT), and designed to measure the sunlight upwelling from the earth's atmosphere in different viewing geometries in the UV, visible and near infrared region (240-2380 nm) to retrieve the amounts and global distribution of the atmospheric trace gases (Bovensmann et al., 1999). Compared to the limited spatial resolution of only $40\times320\,km^2$ with GOME (Global Ozone Monitoring Experiment), SCIAMACHY has a better spatial resolution of $30\times30\,km^2$ to $30\times240\,km^2$ (typically $30\times60\,km^2$), which is of great importance to accurately detect the enhanced NO_2

amount over some hot spots, which are always smoothed out in the GOME data (Beirle et al., 2004). The global coverage is achieved after every 6 days at the equator.

The detail spectral analysis method of SCIAMACHY data can be found in Leue et al. (2001) and Beirle et al. (2003). The NO_2 columns were retrieved in the spectral window between 425–450 nm (channel 3). In order to separate the stratospheric NO_2 column, here the slant columns measured over the Pacific Ocean at the same latitude were taken as the stratospheric NO_2 background values, which were subtracted from the total slant columns to obtain the tropospheric NO_2 SCD. Then, the tropospheric NO_2 VCD was derived by dividing the tropospheric SCD by the corresponding tropospheric AMF (Richter and Burrows, 2002). Here, the AMF was also calculated through TRACY-II with the following settings: for NO_2 a profile was assumed with 80% of the tropospheric column located between the surface and 1 km altitude (homogenous concentration) and the remaining 20% in the free troposphere from 1–15 km (constant mixing ratio); an aerosol layer of 1 km thickness, 0.5 km^{-1} extinction, asymmetry parameter 0.68, and single scattering albedo 0.9 was chosen; the ground albedo was set to 5%. AMF according to these settings were first modeled separately for cloud free and clouded scenes for different cloud top height (CTH). For the clouded scenes, simplified assumptions on the cloud properties were made (vertical extension of the cloud: 1 km, single scattering albedo: 1, asymmetry parameter: 0.85). In the second step, the actual AMF for a given observation was calculated by weighting the AMF for the clear and cloudy parts according to the effective cloud fraction (CF) given for the observation, and the modeled radiances of the clear and cloud parts, respectively. The effective cloud fraction and cloud top height were taken from the FRESCO (Fast Retrieval Scheme for Cloud Observables) algorithm (Koelemeijer et al., 2001, 2002). The errors of the tropospheric NO_2 VCD derived in this way were estimated to be $1\times10^{15}\pm30\%$, which was adopted in the orthogonal regression analysis below.

It should be noted that, though the parameter setting for SCIAMACHY tropospheric AMF simulation does not completely agree with that used in ground-based tropospheric AMF simulation, which takes the seasonal variation into account, the differences would

not cause large deviation to the deduced tropospheric VCD, considering the magnitude of tropospheric AMF in cloud free condition (close to 1). However, especially for clouded scenes and heavy aerosol loads, the choice of the tropospheric NO_2 profile shape has a stronger impact on the satellite AMF than for ground-based observation. The influence of the cloud properties on the comparison between ground-based and satellite data is investigated in more detail in Sect. 4.2.2.

The SCIAMACHY pixels used here are those covering the ground-based experimental site (31.3° N, 121.5° E). Considering the impact of cloud on the observation of trace gases below cloud top, we separate the data measured under the cloud fraction higher and lower than 0.2 (cloudy and clear-sky conditions, respectively), and focus on the latter in the comparison with zenith-sky observation.

4.2.2 Comparison between tropospheric NO_2 VCD from SCIAMACHY and ground-based measurements

In order to compare with SCIAMACHY observation results, the one-hour average tropospheric NO_2VCD from zenith-sky measurement during 10:00~11:00 LT were used, which were observed around the time of SCIAMACHY overpass (SCIAMACHY's overpass over Shanghai for the coincidences was found about 10:20 LT). Figure 13a shows the orthogonal regression of tropospheric NO_2 VCD from SCIAMACHY and zenith-sky measurements under all cloud fractions in 2007 (data from 45 days), with a relative low correlation (the black line, R=0.65). The separate regression analysis for data under clear-sky and cloudy conditions (the data colored red and blue respectively in Fig. 13a) is also performed, which shows better correlation for the former (R=0.68) and worse correlation for the latter (R=0.59).

Since the correlation between the two measurements is not improved much when only the data under clear-sky condition are taken into account, we take a closer look at the corresponding days. It is found that there are more than half of the days (15 days) in which the FRESCO cloud top height (CTH) in the target SCIAMACHY pixels are below 1 km. These cases cannot be processed in the usual way in data retrieval, in which the

ACPD
8, 16713–16762, 2008

model cloud is 1 km thick. Reason for CF>0 and CTH<1 km could be aerosol layers; hence these scenes (as long as cloud fraction was below 0.2) were all treated as if they were cloud free with a homogenous aerosol layer. Depending on the actual scene, the true AMF could be high (due to the multiple scattering within a scattering aerosol layer, or low cloud in the polluted layer) or low (in case of absorbing aerosol or pollution below cloud). Therefore, the tropospheric NO_2 VCD from SCIAMACHY (having AMF of about ~1.2 for these scenes) could be over- or underestimated. Considering the uncertainties of satellite data for days with CF<0.2 and CTH<1 km, we marked those data and analyzed the correlation for the left clear-sky data (days with CF<0.2 and CTH>1 km). As shown in Fig. 13b, the correlation is greatly improved (R=0.86) when the days with CTH <1 km are excluded.

Figure 13c shows the comparison between tropospheric NO_2 VCD from SCIAMACHY and zenith-sky measurements under clear-sky condition (CF<0.2). The data for days with CTH<1 km are also marked. The relative variations of the two data sets match well, while the absolute values of tropospheric NO_2 VCD from zenith-sky measurement are 1.73±0.68 times as large as those retrieved from SCIAMACHY data.

Additionally, we investigate the correlation between the tropospheric NO_2 VCD from SCIAMACHY measurement and the NO_2 surface concentration measured by long-path DOAS observation, which has been performed as a satellite data validation method in previous studies (see e.g. Petritoli et al., 2004). The correlation coefficient for data under clear-sky condition is 0.62, and that for data with CF<0.2 and CTH>1 km is 0.73, both of which are worse than the correlation between tropospheric NO_2 VCD from SCIAMACHY and zenith-sky measurements. This finding also demonstrates the advantage of our VCD_{tropo_zenith} for satellite validation. It should be noted that the correlation results for the surface concentration measurement are still rather good, which is probably related to the fact that during the time of satellite overpass, the PBL over Shangai is relatively stable (see Fig. 8). Satellite validation using surface concentration data at other times of the day, seasons, or locations, will probably be more affected by variations in the PBL and vertical mixing.

ACPD
8, 16713–16762, 2008

4.2.3 Discussion

Unlike Sects. 3.1.4 and 4.1.1, which focus on the errors of tropospheric NO_2 VCD from zenith-sky measurement, in this section, the reasons for the deviation between data from SCIAMACHY and zenith-sky measurements are discussed, with the focus on the errors of satellite data. In general, the most important sources of error in tropospheric NO_2 retrieval from SCIAMACHY data arise from the parameter settings in the calculation of tropospheric AMF. Besides the errors caused by the determination of stratospheric column and surface albedo, which have been discussed in Richter and Burrows (2002), the different assumptions on the distribution of tropospheric NO_2 column, as well as the aerosol single scattering albedo of satellite and zenith-sky AMF simulations in this study also account for the deviation of the final comparison. Here it is interesting to note that the AMF for satellite observation are much stronger affected by these assumptions, especially for (partly) clouded scenes. As mentioned before, the tropospheric AMF used to deduce VCD_{tropo_zenith} were modeled under the assumption that all the tropospheric NO_2 are located within PBL, which varies according to different seasons. However, in the calculation of SCIAMACHY AMF, only 80% of the tropospheric NO_2 column was assumed to be located between 0–1 km altitude. In order to investigate the impact of such different assumptions, we re-calculate the tropospheric NO_2 VCD from SCIAMACHY with 95% of the tropospheric NO_2 column located between 0–1 km. The results are mostly 15% larger than the old ones under clear-sky condition, with a few columns enhanced by a higher percentage. Thus, the absolute values of the new satellite tropospheric VCD are closer to that of the VCD_{tropo_zenith}. The correlation between satellite tropospheric VCD under these two distribution assumptions and the VCD_{tropo_zenith} are presented in Table 3 for different cloud conditions. The correspondence between the tropospheric NO_2 VCD from satellite and zenith-sky measurements is slightly improved by the use of the new distribution assumption, but cannot explain the major part of the deviation between the two data sets.

ACPD
8, 16713–16762, 2008

Additionally, as have been shown in Fig. 10c, the tropospheric AMF deduced with aerosol single scattering albedo set to 1 are 15% larger than that with 0.9 single scattering albedo for the SZA of SCIAMACHY overpass (lower than 60°). Since 0.95 is probably the most realistic value of aerosol single scattering albedo, the derived tropospheric NO_2 VCD from zenith-sky measurement (with SSA assumed to be 1) are probably systematically too low, while that from SCIAMACHY observation (with SSA assumed to be 0.9) are probably too high. Therefore, the correction of aerosol single scattering albedo settings would even enlarge the deviation between the two data sets. Again it should be noted that the effects of different aerosol settings are stronger for the satellite AMF compared to the AMF for zenith-sky observation.

After excluding the possibilities of the above two error sources as the main reasons for the deviation between satellite and zenith-sky tropospheric VCD, we finally turn to the difference of spatial resolution between the two measurements. According to Ordóñez et al. (2006), the agreement between the tropospheric NO_2 VCD from satellite and ground-based in situ measurements in slightly polluted stations was better than that in heavily polluted or average polluted stations. Since our experimental site suffers from heavy traffic pollution, strong spatial gradients are to be expected over the urban site, which cannot be resolved by the satellite observation. Thus the satellite observation should yield systematically lower values compared to those from zenith-sky measurement. In order to further demonstrate this effect, we investigate the spatial gradients around Shanghai to estimate the expected difference of zenith-sky versus satellite columns due to the extent of the satellite pixels ($30\times60\,km^2$). Figure 14 shows the spatial distribution of NO_2 and light pollution around Shanghai. The NO_2 data are average tropospheric VCD from SCIAMACHY observation for 2007 with cloud fraction below 0.2. The light data are measurements from the "Defense Meteorological Satellite Program" DMSP-OLS (Nighttime Lights are for the year 2003) (Cinzano et al., 2001). The number in the title gives the "spatial averaging effect", i.e. the ratio of the maximum at Shanghai and the mean of the satellite observations at a resolution of $30\times60\,km^2$ (according to our selection criterion, see Sect. 4.2.1). Like for the NO_2 data them-

selves, the spatial averaging effect can also be quantified in a similar way for the light data. From the NO_2 measurements we find a ratio of 1.30, which can be regarded as the lower bound of the spatial sampling effect, because the NO_2 gradients were measured with the coarse spatial resolution of the satellite itself. In contrast, the light pollution at night might be a more realistic proxy for NO_x sources, as it was measured at higher spatial resolution. Hence, from the light pollution, we find a value of 1.46, which can be regarded as the upper bound of the spatial averaging effect. Therefore, the difference of zenith-sky versus satellite columns caused by spatial sampling effect ranges from 1.30 to 1.46, which can account for the main part of the deviation between the presented data sets.

To sum up, considering the pollution level of the experimental site, the difference of spatial resolution between the satellite and ground-based observations, as well as the errors of both measurements, the present agreement level is rather good. In order to further validate the satellite measurement, it is necessary to extend the observation of zenith-sky DOAS measurement to the areas with different pollution levels to cover the whole footprint of satellite measurement. Also more detailed information on the tropospheric NO_2 profile would limit the uncertainties; such information could be e.g. derived from Multi-AXis-(MAX-)DOAS observations.

5 Conclusions

A new method to extract the tropospheric NO_2 VCD from ground-based zenith-sky DOAS measurement is presented here. During one year period, both the zenith-sky scattered sunlight observation and the long-path DOAS measurement were carried out simultaneously in Shanghai, China (31.3° N, 121.5° E). The former provided the NO_2 total columns in the daytime, while the latter provided the information of NO_2 surface concentration. By using a three-step strategy, the tropospheric NO_2 VCD was derived (VCD_{tropo_zenith}), which is an important quantity for the estimation of emissions and for the validation of satellite observation. The error analysis showed the accuracy of the

ACPD
8, 16713–16762, 2008

tropospheric NO_2 VCD derived by this extraction method is typically <20% for SZA below 85°.

The NO_2 surface concentration measured by long-path DOAS was also converted into tropospheric VCD ($VCD_{tropo\_surface}$) by multiplying the assumed seasonal PBL height. The comparison between the hourly-averaged $VCD_{tropo\_surface}$ and VCD_{tropo_zenith} provides a deeper insight on the influence of PBL height variation on the tropospheric NO_2 VCD derived from surface concentration. It's concluded that the VCD_{tropo_zenith} is more reliable and suitable for satellite data validation.

A comparison between the tropospheric NO_2 VCD from SCIAMACHY and zenith-sky measurements was made. The relative variations of the two data sets under clear-sky condition (cloud fraction below 0.2) correspond well, while the absolute values of VCD from zenith-sky measurement are on average 1.73 times as large as those from SCIAMACHY observation. The best correlation is found for observations with CF<0.2 and CTH>1 km (R=0.86).

Reasons for the deviation of comparison results were explored, including the assumptions on the distribution of tropospheric NO_2 column, the aerosol single scattering albedo, as well as the difference of spatial resolution between the satellite and ground-based observations. It's concluded that the "spatial averaging effect" can account for a large part of the difference between zenith-sky and satellite columns. Since over Shanghai the distribution of pollution within the SCIAMACHY footprint shows typically strong and systematic gradients (with the maximum close to the measurement site of the ground-based observation), the satellite observation would fail to reproduce the high NO_2 amounts over the polluted experimental site. Therefore, in order to further validate the satellite measurement, the extension of ground-based zenith-sky DOAS measurement is demanded to cover the areas with different pollution levels and the whole satellite footprint.

Acknowledgements. We would like to thank the European Space Agency (ESA) operation center in Frascati (Italy) and the "Deutsches Zentrum für Luft- und Raumfahrt" (DLR, Germany) for making the satellite spectral data available. Information on effective cloud fraction and cloud

top height was taken from the FRESCO algorithm (see http://www.temis.nl/fresco/fresco.html). We are also thankful for the planetary boundary layer height data provided by P. Jöckel from the Max-Planck-Institute for Chemistry, Mainz, Germany. Helpful discussions with A. Richter from the University of Bremen and U. Platt from Heidelberg University are acknowledged. The radiative transfer calculations were performed using the TRACY-II model mainly developed in the satellite group of MPI, Mainz by T. Deutschmann. The WinDOAS spectral analysis software was developed by C. Fayt and M. van Roozendael in IASB/BIRA Uccle, Belgium. The McLinden climatology in SCIATRAN database used to calculate stratospheric NO_2 AMF is also acknowledged. The DMSP-OLS Nighttime Lights data were processed by NOAA's National Geophysical Data Center, and the DMSP data were collected by US Air Force Weather Agency.

References

Bassford, M. R., McLinden, C. A., and Strong, K.: Zenith-sky observations of stratospheric gases: the sensitivity of air mass factors to geophysical parameters and the influence of tropospheric clouds, J. Quant. Spectrosc. Ra., 68, 657–677, 2001.

Beirle, S., Platt, U., Wenig, M., and Wagner, T.: Weekly cycle of NO_2 by GOME measurements: a signature of anthropogenic sources, Atmos. Chem. Phys., 3, 2225–2232, 2003, http://www.atmos-chem-phys.net/3/2225/2003/.

Beirle, S., Platt, U., Wenig, M., and Wagner, T.: Highly resolved global distribution of tropospheric NO_2 using GOME narrow swath mode data, Atmos. Chem. Phys., 4, 1913–1924, 2004, http://www.atmos-chem-phys.net/4/1913/2004/.

Boersma, K. F., Eskes, H. J., and Brinksma, E. J.: Error analysis for tropospheric NO_2 retrieval from space, J. Geophys. Res., 109, D04311, doi:10.1029/2003JD003962, 2004.

Bovensmann, H., Burrows, J. P., Buchwitz, M., Frerick, J., Noël, S., Rozanov, V. V., Chance, K. V., and Goede, A. P. H.: SCIAMACHY: Mission Objectives and Measurement Modes, J. Atmos. Sci., 56(2), 127–150, 1999.

Brinksma, E. J., Pinardi, G., Braak, R., Volten, H., Richter, A., Schönhardt, A., van Roozendael, M., Fayt, C., Hermans, C., Dirksen, R. J., Vlemmix, T., Berkhout, A. J. C., Swart, D. P. J., Oetjen, H., Wittrock, F., Wagner, T., Ibrahim, O. W., de Leeuw, G., Moerman, M., Curier, R. L., Celarier, E. A., Knap, W. H., Veefkind, J. P., Eskes, H. J., Allaart, M., Rothe, R., Piters, A.

J. M., and Levelt, P. F.: The 2005 and 2006 DANDELIONS NO_2 and aerosol intercomparison campaigns, J. Geophys. Res., 113, D16S46, doi:10.1029/2007JD008808, 2008.

Burrows, J. P., Dehn, A., Deters, B., Himmelmann, S., Richter, A., Voigt, S., and Orphal, J.: Atmospheric remote-sensing reference data from GOME: part 1. Temperature-dependent absorption cross sections of NO_2 in the 231–794 nm range, J. Quant. Spectrosc. Ra., 60(6), 1025–1031, 1998.

Burrows, J. P., Richter, A., Dehn, A., Deters, B., Himmelmann, S., Voigt, S., and Orphal, J.: Atmospheric remote-sensing reference data from GOME – Part 2: Temperature-dependent absorption cross sections of O_3 in the 231–794 nm range, J. Quant. Spectrosc. Ra., 61, 509–517, 1999a.

Burrows, J. P., Weber, M., Buchwitz, M., Rozanov, V. V., Ladstätter-Weißenmayer, A., Richter, A., De Beek, R., Hoogen, R., Bramstedt, K., Eichmann, K. U., Eisinger, M., and Perner, D.: The Global Ozone Monitoring Experiment (GOME): Mission concept and first scientific results, J. Atmos. Sci., 56(2), 151–175, 1999b.

Cantrell, C. A.: Technical Note: Review of methods for linear least-squares fitting of data and application to atmospheric chemistry problems, Atmos. Chem. Phys. Discuss., 8, 6409–6436, 2008, http://www.atmos-chem-phys-discuss.net/8/6409/2008/.

Celarier, E. A., Brinksma, E. J., Gleason, J. F., Veefkind, J. P., Cede, A., Herman, J. R., Ionov, D., Goutail, F., Pommereau, J. -P., Lambert, J. -C., van Roozendael, M., Pinardi, G., Wittrock, F., Schönhardt, A., Richter, A., Ibrahim, O. W., Wagner, T., Bojkov, B., Mount, G., Spinei, E., Chen, C. M., Pongetti, T. J., Sander, S. P., Bucsela, E. J., Wenig, M. O., Swart, D. P. J., Volten, H., Kroon, M., and Levelt, P. F.: Validation of Ozone Monitoring Instrument nitrogen dioxide columns, J. Geophys. Res., 113, D15S15, doi:10.1029/2007JD008908, 2008.

Cinzano, P, Falchi, F., and Elvidge, C. D.: The first world atlas of the artificial night sky brightness, Mon. Not. R. Astron. Soc., 328, 689–707, 2001.

Deutschmann, T. and Wagner, T.: TRACY-II Users manual, University of Heidelberg, Heidelberg, Germany, 2006.

Duan, J. and Mao, J. T.: Study on the distribution and variation trends of atmospheric aerosol optical depth over the Yangtze River Delta, Acta Scientiae Circumstantiae, 27(4), 537–543, 2007.

EUMETSAT: GOME-2 Products Guide, available at: http://oiswww.eumetsat.org/WEBOPS/eps-pg/GOME-2/GOME2-PG-index.htm, last access 19 June 2008.

Fayt, C. and v. Roozendael, M.: WinDOAS 2.1 software user manual, IASB/BIRA Uccle, Belgium, 2001.

Greenblatt, G. D., Orlando, J. J., Burkholder, J. B., and Ravishankara, A. R.: Absorption measurements of oxygen between 330 and 1140 nm, J. Geophys. Res., 95, 18 577–18 582, 1990.

Heue, K.-P., Richter, A., Bruns, M., Burrows, J. P., von Friedeburg, C., Platt, U., Pundt, I., Wang, P., and Wagner, T.: Validation of SCIAMACHY tropospheric NO_2-columns with AMAXDOAS measurements, Atmos. Chem. Phys., 5, 1039–1051, 2005, http://www.atmos-chem-phys.net/5/1039/2005/.

Hönninger, G. and Platt, U.: The role of BrO and its vertical distribution during surface ozone depletion at Alert, Atmos. Environ., 36, 2481–2489, 2002.

Institute of Remote Sensing University of Bremen, Germany: User's guide for the software package SCIATRAN (Radiative Transfer Model and Retrieval Algorithm), version 2.0, available at: http://www.iup.uni-bremen.de/sciatran/downloads, last access 19 June 2008, 2004.

Ionov, D., Goutail, F., Pommereau, J. -P, and Bazureau, A.: Ten years of NO_2 comparisons between ground-based SAOZ and satellite instruments (GOME, SCIAMACHY, OMI), in: Proceedings of Atmospheric Science Conference, ESRIN, Frascati, Italy, 8–12 May 2006, CD-ROM. p. 16.1, 2006a.

Ionov, D., Sinyakov, V. P., and Semenov, V. K.: Validation of GOME (ERS-2) NO_2 vertical column data with ground-based measurements at Issyk-Kul (Kyrgyzstan), Adv. Space Res., 37(12), 2254–2260, 2006b.

Jöckel, P., Tost, H., Pozzer, A., Brühl, C., Buchholz, J., Ganzeveld, L., Hoor, P., Kerkweg, A., Lawrence, M. G., Sander, R., Steil, B., Stiller, G., Tanarhte, M., Taraborrelli, D., van Aardenne, J., and Lelieveld, J.: The atmospheric chemistry general circulation model ECHAM5/MESSy1: consistent simulation of ozone from the surface to the mesosphere, Atmos. Chem. Phys., 6, 5067–5104, 2006, http://www.atmos-chem-phys.net/6/5067/2006/.

Koelemeijer, R. B. A., Stammes, P., Hovenier, J. W., and de Haan, J. F.: A fast method for retrieval of cloud parameters using oxygen A band measurements from the Global Ozone Monitoring Experiment, J. Geophys. Res., 106(D4), 3475–3490, 2001.

Koelemeijer, R. B. A., Stammes, P., Hovenier, J. W., and de Haan, J. F.: Global distributions of effective cloud fraction and cloud top pressure derived from oxygen A band spectra measured by the Global Ozone Monitoring Experiment: comparison to ISCCP data, J. Geophys.

Res., 107(D12), 4151, doi:10.1029/2001JD000840, 2002.
Kraus, S.: DOASIS, DOAS for Windows software, in: Proceedings of the 1st International DOAS-Workshop, Heidelberg, Germany, 13–14 September, CD-ROM, 2001.
Lambert, J.-C., Granville, J., Allaart, M., Blumenstock, T., Coosemans, T., De Mazière, M., Friess, U., Gil, M., Goutail, F., Ionov, D. V., Kostadinov, I., Kyrö, E., Petritoli, A., Piters, A., Richter, A., Roscoe, H. K., Schets, H., Shanklin, J. D., Soebijanta, V. T., Suortti, T., van Roozendael, M., Varotsos, C., and Wagner, T.: Ground-based comparisons of early SCIAMACHY O_3 and NO_2 columns, in: Proceedings of the First ENVISAT Validation Workshop, ESA/ESRIN, Frascati, Italy, 9–13 December 2002, ESA SP-531, 2003.
Leue, C., Wenig, M., Wagner, T., Klimm, O., Platt, U., and Jähne, B.: Quantitative analysis of NO_x emissions from Global Ozone Monitoring Experiment satellite image sequences, J. Geophys. Res., 106(D6), 5493–5506, 2001.
Levelt, P. F. and Noordhoek, R.: OMI Algorithm Theoretical Basis Document, Volume 1: OMI Instrument, Level 0-1b Processor, Calibration and Operations, Tech. Rep. ATBD-OMI-01, Version 1.1, 2002.
Meena, G. S., Bhosale, C. S., and Jadhav, D. B.: Influence of tropospheric clouds on ground-based measurements of stratospheric trace gases at Tropical station, Pune, Atmos. Environ., 38(21), 3459–3468, 2004.
Noxon, J. F.: Nitrogen dioxide in the stratosphere and troposphere measured by ground-based absorption spectroscopy, Science, 189, 547–549, 1975.
Ordóñez, C., Richter, A., Steinbacher, M., Zellweger, C., Nüβ, H., Burrows, J. P., and Prévôt, A. S. H.: Comparison of 7 years of satellite-borne and ground-based tropospheric NO_2 measurements around Milan, Italy, J. Geophys. Res., 111, D05310, doi:10.1029/2005JD006305, 2006.
Perner, D. and Platt, U.: Absorption of light in the atmosphere by collision pairs of oxygen $(O_2)_2$, Geophys. Res. Lett., 7(12), 1053–1056, 1980.
Petritoli, A., Bonasoni, P., Giovanelli, G., Ravegnani, F., Kostadinov, I., Bortoli, D., Weiss, A., Schaub, D., Richter, A., and Fortezza, F.: First comparison between ground-based and satellite-borne measurements of tropospheric nitrogen dioxide in the Po basin, J. Geophys. Res., 109, D15307, doi:10.1029/2004JD004547, 2004.
Pfeilsticker, K., Erle, F., Funk, O., Marquard, L., Wagner, T., and Platt, U.: Optical path modifications due to tropospheric clouds: implications for zenith sky measurements of stratospheric gases, J. Geophys. Res., 103(D19), 25 323–25 335, 1998.

Platt, U.: Differential optical absorption spectroscopy (DOAS), in: Air Monitoring by Spectroscopic Techniques, Chemical Analysis Series, Vol. 127, edited by: Sigrist, M. W., John Wiley and Sons, New York, USA, 1994.

Pommereau, J. -P. and Goutail, F.: O_3 and NO_2 ground-based measurements by visible spectrometry during arctic winter and spring 1988, Geophys. Res. Lett., 15, 891–894, 1988.

Richter, A. and Burrows, J. P.: Tropospheric NO_2 from GOME measurements, Adv. Space Res., 29(11), 1673–1683, 2002.

Richter, A., Burrows, J. P., Nüß, H., Granier C., and Niemeier, U.: Increase in tropospheric nitrogen dioxide over China observed from space, Nature, 437, 129–132, 2005.

Rothman, L. S., Rinsland, C. P., Goldman, A., Massie, S. T., Edwards, D. P., Flaud, J.-M., Perrin, A., Camy-Peyret, C., Dana, V., Mandin, J. -Y., Schroeder, J., McCann, A., Gamache, R. R., Wattson, R. B., Yoshino, K., Chance, K. V., Jucks, K. W., Brown, L. R., Nemtchinov, V., and Varanasi, P.: The HITRAN molecular spectroscopic database and HAWKS (HITRAN atmospheric workstation): 1996 edition, J. Quant. Spectrosc. Ra., 60(5), 665–710, 1998.

Van Roozendael, M., Hermans, C., De Mazière, M., and Simon, P. C.: Stratospheric NO_2 observations at the Jungfraujoch Station between June 1990 and May 1992, Geophys. Res. Lett., 21(13), 1383–1386, 1994.

Wagner, T., Erle, F., Marquard, L., Otten, C., Pfeilsticker, K., Senne, T., Stutz, J., and Platt, U.: Cloudy sky optical paths as derived from differential optical absorption spectroscopy observations, J. Geophys. Res., 103(D19), 25 307–25 321, 1998.

Wagner, T., von Friedeburg, C., Wenig, M., Otten, C., and Platt, U.: UV-visible observations of atmospheric O_4 absorptions using direct moonlight and zenith-scattered sunlight for clear-sky and cloudy sky conditions, J. Geophys. Res., 107(D20), 4424, doi:10.1029/2001JD001026, 2002.

Wagner, T., Burrows, J. P., Deutschmann, T., Dix, B., von Friedeburg, C., Frieß, U., Hendrick, F., Heue, K.-P., Irie, H., Iwabuchi, H., Kanaya, Y., Keller, J., McLinden, C. A., Oetjen, H., Palazzi, E., Petritoli, A., Platt, U., Postylyakov, O., Pukite, J., Richter, A., van Roozendael, M., Rozanov, A., Rozanov, V., Sinreich, R., Sanghavi, S., and Wittrock, F.: Comparison of box-air-mass-factors and radiances for Multiple-Axis Differential Optical Absorption Spectroscopy (MAX-DOAS) geometries calculated from different UV/visible radiative transfer models, Atmos. Chem. Phys., 7, 1809–1833, 2007, http://www.atmos-chem-phys.net/7/1809/2007/.

Wittrock, F., Oetjen, H., Richter, A., Fietkau, S., Medeke, T., Rozanov, A., and Burrows, J. P.:

MAX-DOAS measurements of atmospheric trace gases in Ny-Ålesund – Radiative transfer studies and their application, Atmos. Chem. Phys., 4, 955–966, 2004, http://www.atmos-chem-phys.net/4/955/2004/.

Yu, Y., Geyer, A., Xie, P., Galle, B., Chen, L. M., and Platt, U.: Observations of carbon disulfide by differential optical absorption spectroscopy in Shanghai, Geophys. Res. Lett., 31, L11107, doi:10.1029/2004GL019543, 2004.

Zhou, B., Hao, N., and Chen, L. M.: Study on the effect of Fraunhofer structure to the measurement of atmospheric pollutants with differential optical absorption spectroscopy, Acta Phys. Sin-Ch Ed., 54(9), 4445–4450, 2005.

Table 1. Seasonal aerosol scenarios for the simulation of tropospheric NO_2 AMF. The asymmetry parameter (0.68) and single scattering albedo (1) were assumed to be constant for all seasons.

Season	Aerosol optical depth (AOD)	Altitude range/ PBL height (km)
Winter (December, January and February)	0.6	0–0.5
Spring (March, April and May)	1	0–0.8
Summer (June, July and August)	1.2	0–1
Autumn (September, October and November)	0.8	0–0.8

ACPD
8, 16713–16762, 2008

Table 2. Tropospheric NO_2 and aerosol settings for different test cases, with aerosol asymmetry parameter set to 0.68 for all cases.

Case	The extension of aerosol layer (km)	The extension of tropospheric NO_2 layer (km)	Aerosol single scattering albedo	AOD
1	0–0.8	0–1	1	1.2
2	0–1	0–1	1	1.2
3	0–1	0–0.8	1	1.2
4	0–0.8	0–0.8	1	1.2
5	0–0.8	0–0.8	0.95	1.2
6	0–0.8	0–0.8	0.9	1.2
7	0–0.8	0–0.8	1	0.4
8	0–0.8	0–0.8	1	0.8
9	0–0.8	0–0.8	1	1.5
10	0–0.3	0–0.3	1	1.2
11	0–0.6	0–0.6	1	1.2

ACPD
8, 16713–16762, 2008

Table 3. Comparison between SCIAMACHY tropospheric VCD under two tropospheric NO_2 distribution assumptions and the VCD_{tropo_zenith}, for different cloud conditions.

Cloud condition	80% of tropospheric NO_2 column located between 0–1 km			95% of tropospheric NO_2 column located between 0–1 km		
	R	Slope	Intercept	*R*	Slope	Intercept
All	0.65	0.58±0.08	−0.25±0.12	0.67	0.73±0.09	−0.19±0.16
Cloudy (CF>0.2)	0.59	0.35±0.09	−0.08±0.12	0.64	0.82±0.18	−0.45±0.28
Clear-sky (CF<0.2)	0.68	0.51±0.09	0.24±0.20	0.67	0.59±0.11	0.29±0.24
Clear-sky (CF<0.2, CTH>1 km)	0.86	0.53±0.13	0.13±0.35	0.83	0.60±0.15	0.27±0.44
Clear-sky (CF<0.2, CTH<1 km)	0.53	0.48±0.14	0.33±0.30	0.54	0.55±0.16	0.34±0.35

ACPD
8, 16713–16762, 2008

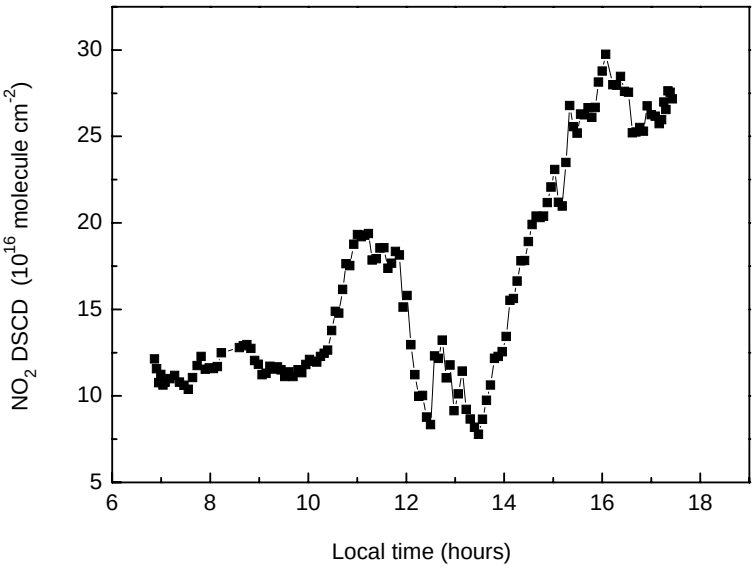

Fig. 1. Perturbation on zenith-sky measurement of NO_2 caused by strong tropospheric NO_x emission (diurnal variation of the NO_2 DSCD on 2 February 2007). Even during twilight period, the measurement was dominated by the tropospheric NO_2 absorption.

ACPD
8, 16713–16762, 2008

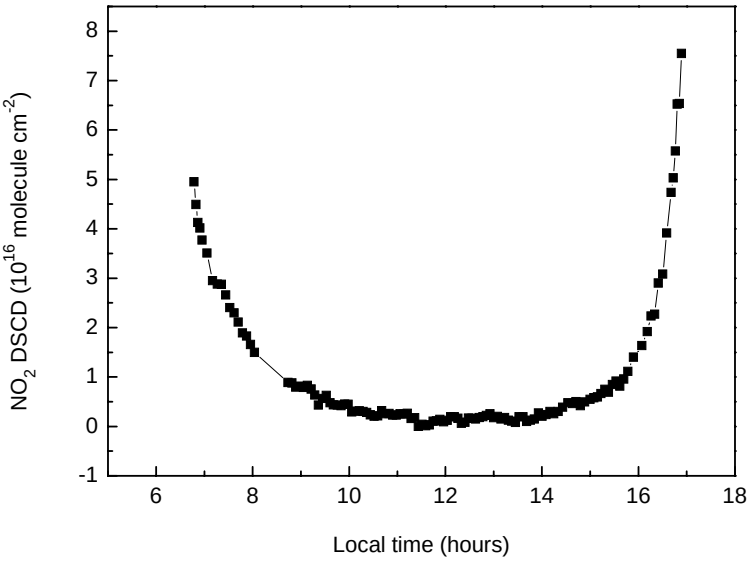

Fig. 2. Example of the diurnal variation of NO_2 DSCD, which was dominated by the stratospheric absorption (observed at Chongming Island on 17 December 2006).

ACPD

8, 16713–16762, 2008

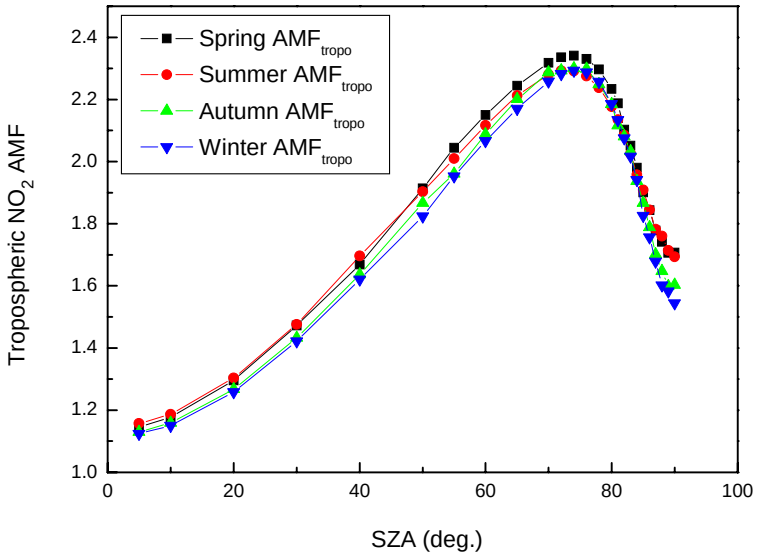

Fig. 3. Tropospheric NO_2 AMF modeled by TRACY-II assuming seasonal NO_2 profiles and aerosol scenarios.

ACPD
8, 16713–16762, 2008

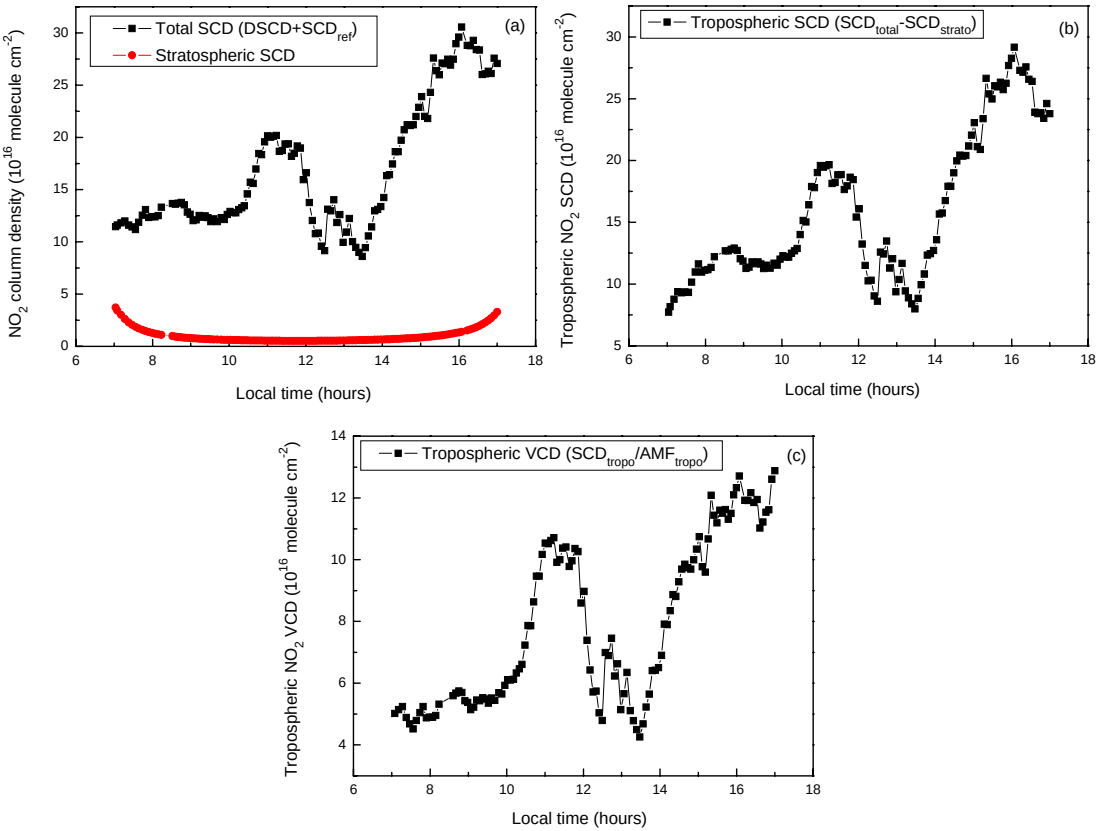

Fig. 4. Extraction of the tropospheric NO_2 VCD from zenith-sky observations. **(a)** Diurnal variation of the total NO_2 SCD and the deduced stratospheric SCD on 2 February 2007; **(b)** tropospheric NO_2 SCD; **(c)** tropospheric NO_2 VCD.

ACPD
8, 16713–16762, 2008

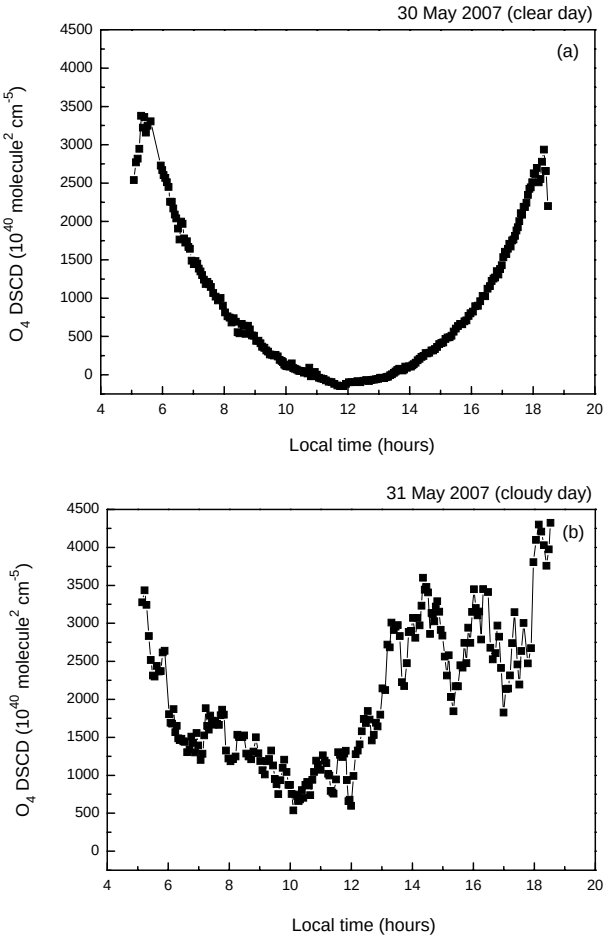

Fig. 5. Diurnal variations of the O_4 DSCD on a clear (30 May 2007), **(a)** and a cloudy day (31 May 2007) **(b)**, respectively.

ACPD
8, 16713–16762, 2008

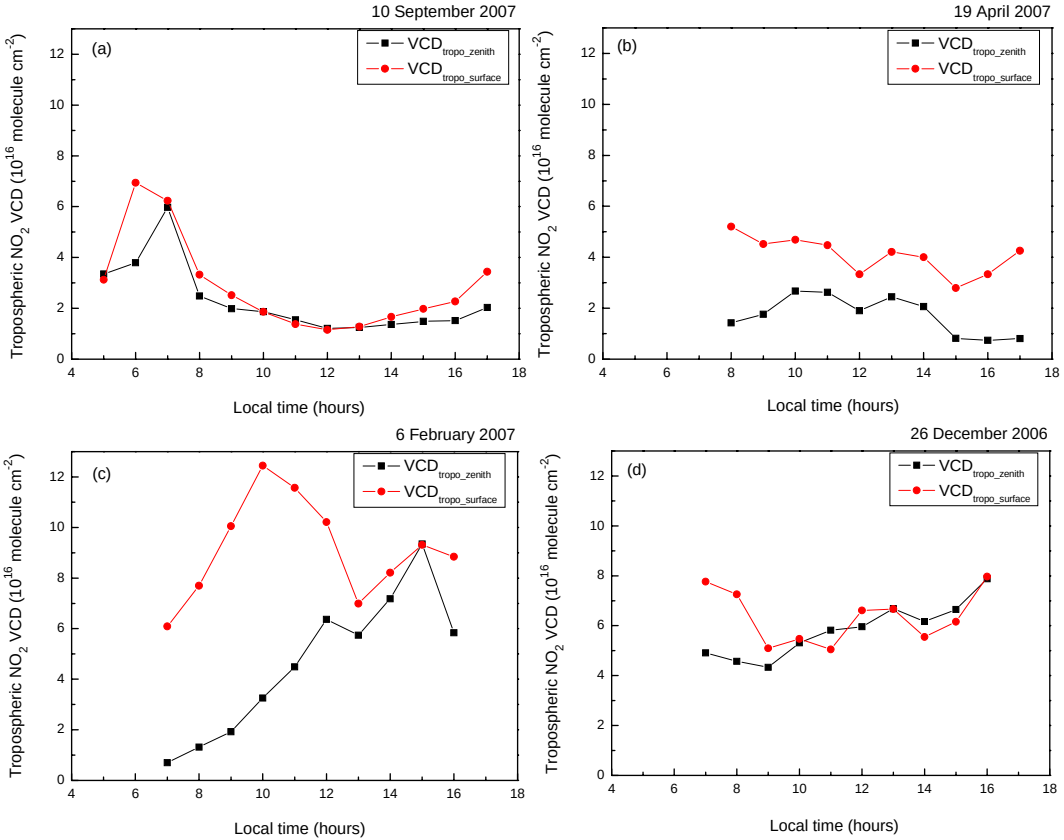

Fig. 6. Typical examples of four groups of comparisons between the tropospheric NO_2 VCD from zenith-sky observation (VCD_{tropo_zenith}) and long-path DOAS observation ($VCD_{tropo\_surface}$).

ACPD
8, 16713–16762, 2008

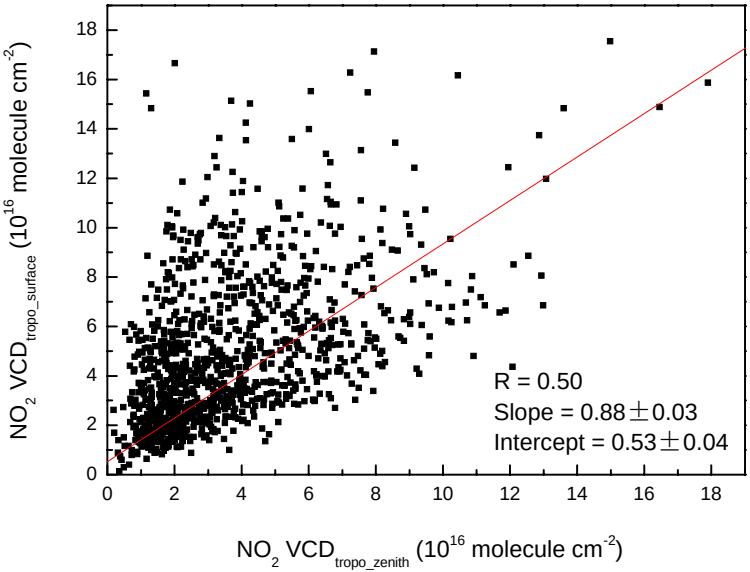

Fig. 7. Regression analysis of the tropospheric NO_2 VCD derived from long-path DOAS observation ($VCD_{tropo\_surface}$) and zenith-sky observation (VCD_{tropo_zenith}) for 98 days under cloud-free condition.

ACPD
8, 16713–16762, 2008

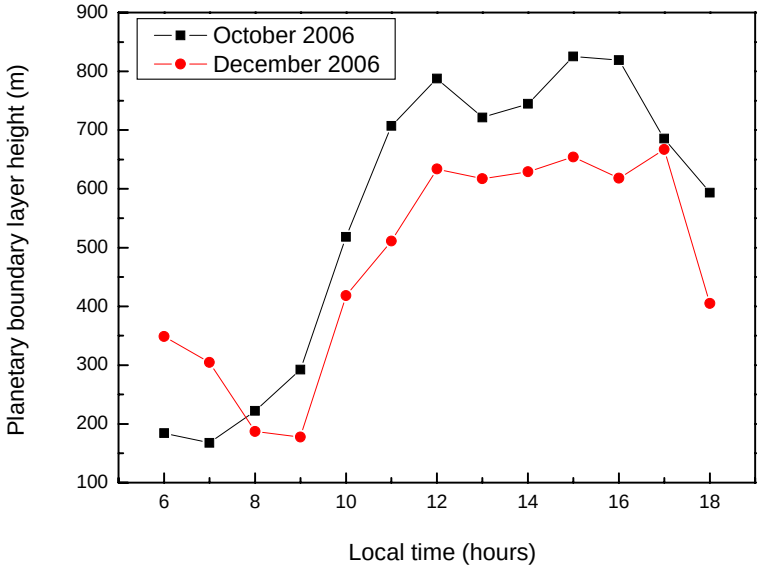

Fig. 8. Monthly-averaged diurnal Planetary Boundary Layer (PBL) height for Shanghai in October and December 2006, modeled and provided by Patrick Jöckel, modeling group at MPI for Chemistry, Mainz, Germany. The model results were taken from the S2 simulation of the Modular Earth Submodel System (MESSy), see Jöckel et al., 2006.

ACPD
8, 16713–16762, 2008

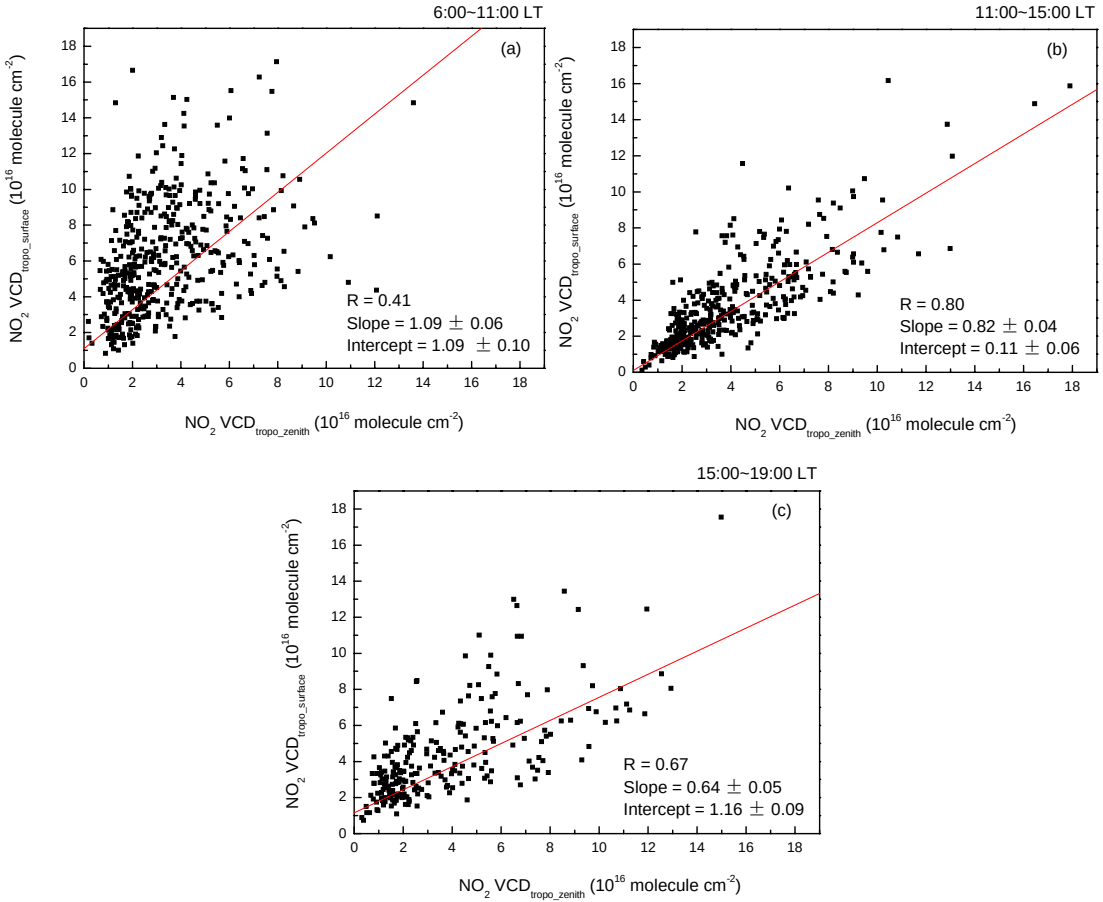

Fig. 9. Regression analysis of the tropospheric NO_2 VCD derived from long-path DOAS observation ($VCD_{tropo\_surface}$) and zenith-sky observation (VCD_{tropo_zenith}) for three selected periods during the daytime (6:00~11:00 LT, 11:00~15:00 LT and 15:00~19:00 LT).

ACPD
8, 16713–16762, 2008

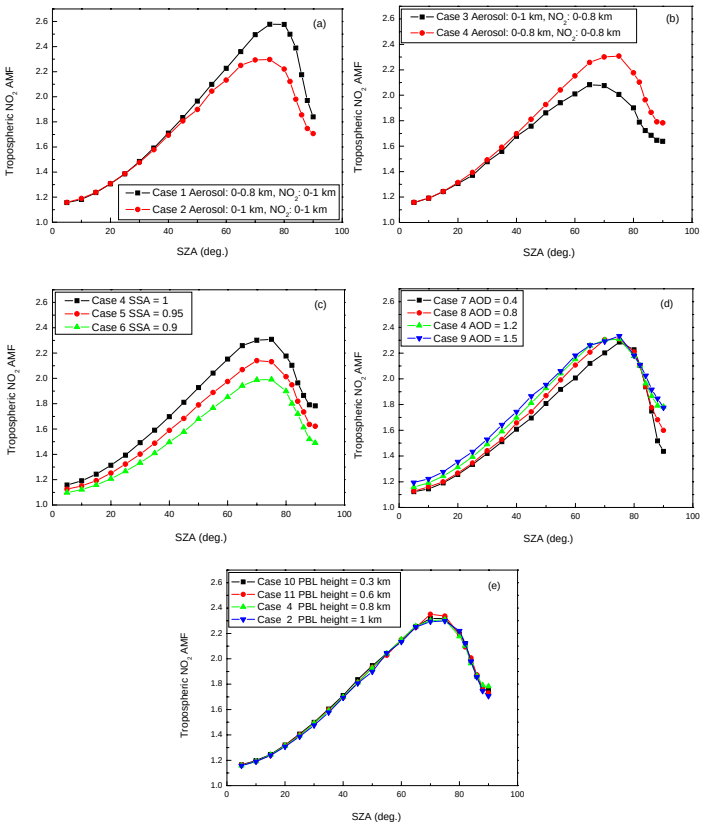

Fig. 10. Case studies of the influence of aerosol settings and profile assumptions on the tropospheric NO_2 AMF modeled by TRACY-II. **(a)** The tropospheric NO_2 AMF deduced under the assumptions that the aerosol layer extends lower and **(b)** higher than the tropospheric NO_2; **(c)** The tropospheric NO_2 AMF deduced under different aerosol single scattering albedo (SSA), **(d)** AOD and **(e)** PBL height assumptions. The concrete parameter settings of each case can be found in Table 2.

ACPD
8, 16713–16762, 2008

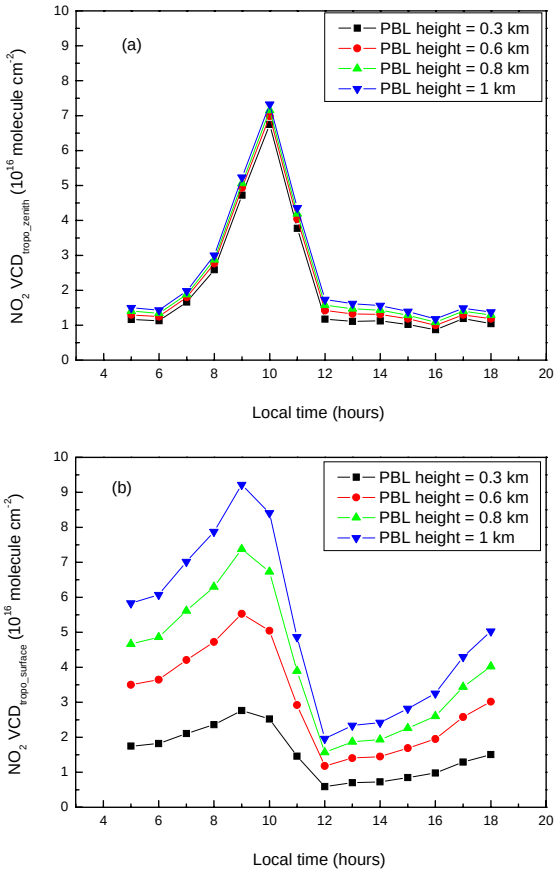

Fig. 11. (a) Corresponding tropospheric NO_2 VCD from zenith-sky observation and **(b)** long-path DOAS observation for 9 June 2007, deduced under the above four PBL height assumptions in Fig. 10e.

ACPD
8, 16713–16762, 2008

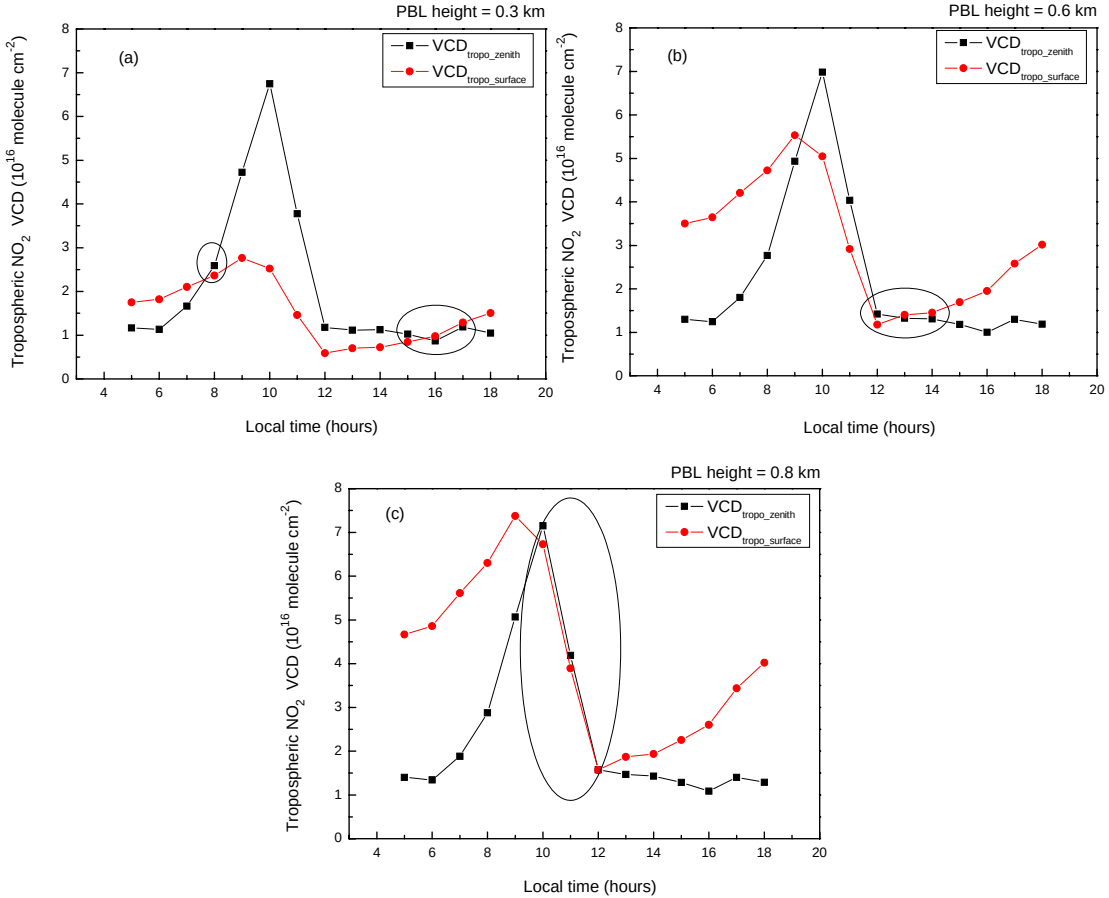

Fig. 12. Comparison between the tropospheric NO_2 VCD derived from zenith-sky observation (VCD_{tropo_zenith}) and long-path DOAS observation ($VCD_{tropo\_surface}$) on 9 June 2007 under different PBL height assumptions. The agreements of two data sets are circled.

ACPD
8, 16713–16762, 2008

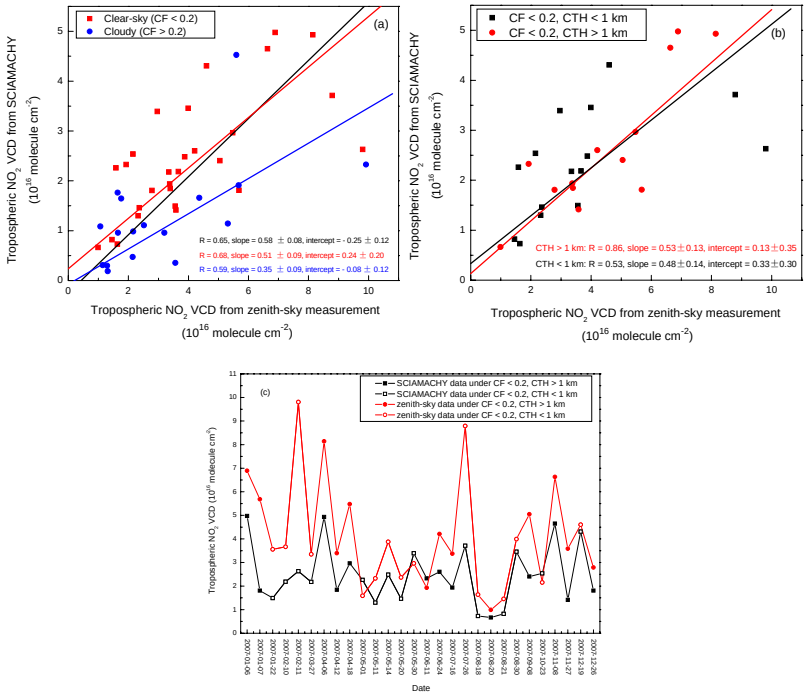

Fig. 13. Comparison between the tropospheric NO_2 VCD deduced from SCIAMACHY and zenith-sky observations. **(a)** Orthogonal regression of the tropopheric NO_2 VCD from SCIAMACHY and zenith-sky measurements under all cloud fractions (the black fitted line). Red points represent the data for days under clear-sky condition, while the blue points represent the data for cloudy days; **(b)** Regression analysis of data for days with CF<0.2 and CTH<1 km (the black points), and CF<0.2 and CTH>1 km (the red points) repectively; **(c)** Comparison between the tropospheric NO_2 VCD from SCIAMACHY and zenith-sky measurements under clear-sky conditions (CF<0.2). Open squares and circles represent the satellite and zenith-sky data points for days with CTH<1 km, respectively.

ACPD
8, 16713–16762, 2008

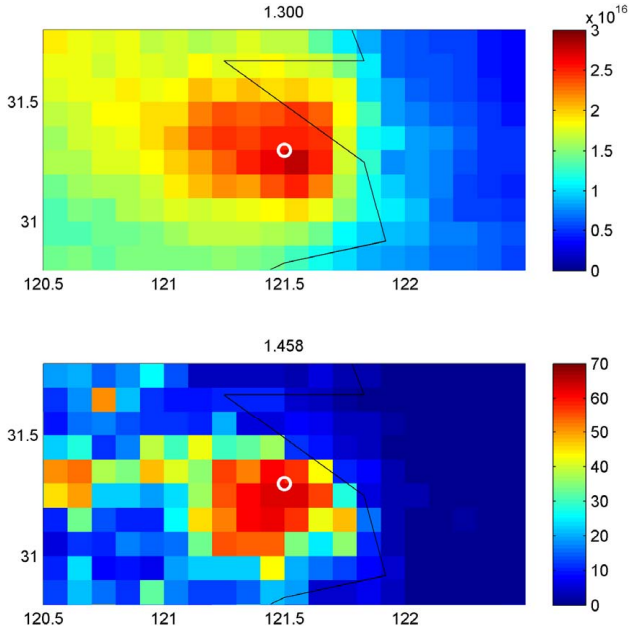

Fig. 14. Spatial distribution of NO_2 (upper) and light (lower) pollution around Shanghai. The NO_2 data are the average tropospheric VCD from SCIAMACHY observation for 2007 with cloud fraction below 0.2. The light data are measurements from the "Defense Meteorological Satellite Program" DMSP-OLS. The number in the title gives the "spatial averaging effect", i.e. the ratio of the maximum at Shanghai and the mean of the satellite observations at a resolution of $30 \times 60\,km^2$. The circle indicates the ground-based experimental site. The black line represents the coastline of the East Sea.